

Lawrence Berkeley National Laboratory

Recent Work

Title

ANALYTICAL AND NUMERICAL STUDY OF ONE-DIMENSIONAL INFILTRATION IN UNSATURATED POROUS MEDIA

Permalink

<https://escholarship.org/uc/item/1c33g6ps>

Authors

R.W
Zimmerman
Bodvarsson, B.S.

Publication Date

1988-07-01



Lawrence Berkeley Laboratory

UNIVERSITY OF CALIFORNIA

EARTH SCIENCES DIVISION

RECEIVED
LAWRENCE
BERKELEY LABORATORY

Submitted to Water Resources Research

SEP 30 1988

LIBRARY AND
DOCUMENTS SECTION

Analytical and Numerical Study of One-Dimensional Infiltration in Unsaturated Porous Media

R.W. Zimmerman and G.S. Bodvarsson

July 1988

For Reference

Not to be taken from this room



LBL-25629
c.1

DISCLAIMER

This document was prepared as an account of work sponsored by the United States Government. While this document is believed to contain correct information, neither the United States Government nor any agency thereof, nor the Regents of the University of California, nor any of their employees, makes any warranty, express or implied, or assumes any legal responsibility for the accuracy, completeness, or usefulness of any information, apparatus, product, or process disclosed, or represents that its use would not infringe privately owned rights. Reference herein to any specific commercial product, process, or service by its trade name, trademark, manufacturer, or otherwise, does not necessarily constitute or imply its endorsement, recommendation, or favoring by the United States Government or any agency thereof, or the Regents of the University of California. The views and opinions of authors expressed herein do not necessarily state or reflect those of the United States Government or any agency thereof or the Regents of the University of California.

Analytical and Numerical Study of One-Dimensional Infiltration in Unsaturated Porous Media

Robert W. Zimmerman

Gudmundur S. Bodvarsson

Earth Sciences Division
Lawrence Berkeley Laboratory
University of California
Berkeley, CA 94720

One-dimensional infiltration of water into an unsaturated porous medium is studied, using various analytical and numerical techniques. One method of solution utilizes a variation of the Boltzmann transformation, reducing the governing PDE to a two-point ODE boundary-value problem. Numerical integration shows that the instantaneous flux is proportional to $t^{-1/2}$, with a constant of proportionality that depends in a highly nonlinear way on both the boundary potential and the initial saturation. An approximate solution to the governing equation is derived using a "boundary-layer" approach, in which an assumed saturation profile is substituted into the PDE and integrated from the boundary out to the "penetration distance". This method yields closed-form expressions for the penetration distance and the flux at the boundary. The accuracy of this solution depends on the various parameters of the problem, but seems typically to be within 15%.

Introduction

The flow of water through partially saturated rocks or soils poses an interesting and difficult mathematical problem that has applications to various areas of science and technology. The uppermost region of the earth's crust is typically in a partially saturated state that extends down to the water table. This region, known as the unsaturated or "vadose" zone, has a thickness ranging from a few meters to a few hundreds of meters. Historically, the problem of the infiltration of water into an unsaturated medium has been of the most interest to agricultural scientists and groundwater hydrologists. With the proposed use of the upper crust of the earth for the disposal and storage of hazardous wastes, flow in the unsaturated zone has taken on even wider relevance. In this paper, the problem of one-dimensional infiltration of water into an initially unsaturated semi-infinite formation is studied, using both numerical and analytical techniques. While the immediate purpose of this work is for modeling flow in the vicinity of the planned nuclear waste repository at Yucca Mountain in Nevada, the results should be of general applicability to infiltration problems in unsaturated media.

Formulation of Problem

One-dimensional flow of water through a porous rock or soil is governed by the following partial differential equation [Hillel, 1980]:

$$\frac{\partial}{\partial x} \left[\beta k_r(\psi) \frac{\partial \psi}{\partial x} \right] = G(\psi) \frac{\partial \psi}{\partial t} \quad (1)$$

The dependent variable ψ in equation (1) represents the pressure potential of water in the rock; it is positive in regions of full saturation, and negative in regions of partial saturation. When the medium is less than fully saturated, the potential is often referred

to as the capillary pressure. The parameter β represents $k/\mu\phi$, where k and ϕ are the absolute permeability and porosity of the rock, and μ is the dynamic viscosity of water. $k_r(\psi)$ is the relative permeability of the medium to water, and is a dimensionless number lying between zero and one. The storativity function, $G(\psi)$, is defined by $G(\psi) = \partial S / \partial \psi$, where S is the liquid saturation. Equation (1) essentially represents conservation of mass, along with Darcy's law; the left hand side is the divergence of the volumetric flux of water, while the right hand side represents the change in the water content of the medium. Since (1) does not include a gravitational potential term, it can be used to describe horizontal flow, or vertical flow in situations where the potential gradients are large relative to the specific gravity of water.

Each rock formation has its own "characteristic functions", $k_r(\psi)$ and $S(\psi)$, which relate the saturation, capillary pressure, and relative permeability. As a general rule, the relative permeability decreases from one to zero as the saturation varies from some maximum value S_s down to the residual saturation S_r . The capillary pressure will decrease from zero down to $-\infty$ over this range of saturations. These functions reflect the pore size distribution, and other aspects of the pore geometry, and in general must be determined experimentally. Many types of functions have been proposed to represent characteristic curves [Rulon *et al.*, 1986]. The equations of van Genuchten [1980] will be used in this study, although the methods described in this paper can incorporate any set of characteristics curves. The van Genuchten formulae can be written as

$$S(\psi) = S_r + (S_s - S_r)[1 + (\alpha|\psi|)^n]^{-m}, \quad (2)$$

$$k_r(\psi) = \frac{[1 - (\alpha|\psi|)^{n-1}[1 + (\alpha|\psi|)^n]^{-m}]^2}{[1 + (\alpha|\psi|)^n]^{m/2}}, \quad (3)$$

where n and m are two parameters related by $m=(n-1)/n$, and α is a parameter that has a dimension of 1/Pressure. Examples of these characteristic curves are shown in normalized form in Figure 1, with the normalized saturation defined as $\hat{S} = (S - S_r)/(S_s - S_r)$, and the normalized capillary pressure as $\hat{\psi} = \alpha\psi$. The value of α is reflective of the average pore diameter in the rock, with larger values of α corresponding to larger characteristic pore diameters. The parameter n is related to the width of the pore size distribution, with larger values of n corresponding to narrower distributions. For saturated flow, $k_r = 1$, and S is constant, so that $G(\psi) = 0$. In this case, equation (1) merely predicts a constant pressure gradient.

A basic problem in the area of fluid flow in the unsaturated zone is that of infiltration from a planar surface (such as a fracture) filled with water at some potential ψ_w , into a semi-infinite formation which is initially at some uniform saturation S_i . This saturation will correspond (via equation [2]) to some potential ψ_i , where $\psi_i < 0$. For this problem, the appropriate initial and boundary conditions are

$$\psi(x, t = 0) = \psi_i \quad \text{for all } x > 0, \quad (4)$$

$$\psi(x = 0, t) = \psi_w \quad \text{for all } t > 0, \quad (5)$$

$$\lim_{x \rightarrow \infty} \psi(x, t) = \psi_i \quad \text{for all } t > 0. \quad (6)$$

The model represented by equations (1-6) neglects the storativity due to the compressibilities of the water and the pore space of the rock, which generally is negligible compared to $G(\psi)$. Hysteretic effects, wherein the capillary pressure depends not only on the saturation, but also on whether drainage or imbibition is taking place, are likewise ignored. This causes no difficulty for the problem under consideration, since the

saturation at each point will be a monotonic function of time.

Similarity Transformation

Because of the variation of k_r and S with ψ , equations (1-6) represent a highly nonlinear problem that is not amenable to standard analytical techniques such as Laplace transforms, Green's functions, etc. Philip [1960] has derived a closed-form solution to this problem, but this solution requires that the characteristic curves be represented as series of inverse error functions. However, expressing equations (2) and (3) in this form requires considerable computational effort, made particularly difficult by the relative obscurity of inverse error functions. Solutions to this problem are much more readily obtained numerically.

The partial differential equation (1) could be solved directly using finite difference or finite element techniques. An easier method, based on a similarity transformation, reduces the PDE to an ODE, which is considerably easier to solve. The first step in this procedure is to transform (1) into a dimensionless form. This can be accomplished through the following change of variables:

$$\hat{\psi} = \alpha\psi, \quad (7)$$

$$\eta = \left[\frac{\alpha(S_s - S_r)x^2}{\beta t} \right]^{1/2}. \quad (8)$$

This is similar to the traditional Boltzmann transformation $\eta = x/\sqrt{t}$, except that the factor α/β is needed to non-dimensionalize the variable η , while the factor $(S_s - S_r)$ is included so as to simplify subsequent equations as much as possible. This definition is similar to that used by Martinez [1988], except that by using α instead of the initial

capillary pressure for the normalization, it allows a characteristic length scale to be defined independently of the boundary conditions of the problem.

Under this change of variables, equation (1) is transformed into

$$\frac{d}{d\eta} \left[k_r(\hat{\psi}) \frac{d\hat{\psi}}{d\eta} \right] + \frac{\eta}{2} \hat{G}(\hat{\psi}) \frac{d\hat{\psi}}{d\eta} = 0. \quad (9)$$

$\hat{\psi}$ is seen to be a function only of the single similarity variable η , and so equation (9) is an *ordinary* differential equation. The function \hat{G} in (9) is now defined as $d\hat{S}/d\hat{\psi}$, where \hat{S} is the normalized saturation $(S-S_r)/(S_s-S_r)$. The boundary conditions (4-6) are transformed into

$$\hat{\psi}(\eta=0) = \hat{\psi}_w, \quad (10)$$

$$\lim_{\eta \rightarrow \infty} \hat{\psi}(\eta) = \hat{\psi}_i. \quad (11)$$

The two conditions (5) and (6) collapse into the single condition (11), since both $x \rightarrow \infty$ and $t \rightarrow 0$ imply $\eta \rightarrow \infty$. This is necessary for the similarity transformation method to be applicable, since a second-order ODE such as (9) can have only two arbitrary boundary conditions imposed on it.

For given values of $\hat{\psi}_i$ and $\hat{\psi}_w$, equations (9-11) can be solved numerically using a so-called ‘‘shooting’’ technique [Press *et al.*, 1986]. In this method, a value of $d\hat{\psi}/d\eta$ at $\eta=0$ is chosen, and (9) is then integrated as an initial-value problem until $\hat{\psi}$ stabilizes at some value $\hat{\psi}(\infty)$. An iterative root-finding technique can then be used, with $\hat{\psi}(\infty)$ treated as a function of $d\hat{\psi}/d\eta$ at $\eta=0$, to arrive at the proper value of $\hat{\psi}(\infty) = \hat{\psi}_i$. If it is desired merely to generate families of saturation profiles for

different values of $\hat{\psi}_i$, or to study the relationship between $\hat{\psi}_i$ and the flux, these iterations are not necessary, and the problem can be treated as a pure initial value problem. Note that for the purposes of studying the relationship between the initial saturation and the flux, the non-dimensionalization substantially reduces the amount of calculation needed, since the only parameter in (9) that has not been normalized out is the van Genuchten n .

Equation (9) has been integrated for various values of $\hat{\psi}_i$, $\hat{\psi}_w$, and n , using the fourth-order Runge-Kutta scheme [Press *et al.*, 1986]. The n parameter, which reflects the width of the pore-size distribution, is necessarily greater than 1, with typical values being on the order of 2–5 [van Genuchten, 1980; Rulon *et al.*, 1986]. For this range of values, the numerical value of n has only a small effect on the potential profiles, and does not affect any of the main qualitative features of the solution. It is therefore worthwhile to choose a fixed value of n , such as $n = 3$, in order to study the effect of $\hat{\psi}_i$ and $\hat{\psi}_w$. Figure 2 shows pressure profiles for the case $n = 3$, with zero pressure on the boundary (*i.e.*, $\hat{\psi}_w = 0$), and different values of $\hat{\psi}_i$. Since $\hat{\psi}_i = -4$ corresponds to a value of \hat{S}_i of only a few saturation points above irreducible saturation, the initial capillary pressures shown in this figure cover most of the range of interest. Figure 3 shows the profiles for a fixed value of $\hat{\psi}_i = -2$, with different “wall” pressures, $\hat{\psi}_w$. In contrast to a linear diffusion problem [*cf.* Crank, 1975], the distance into the formation to which the pressure disturbance has propagated depends significantly on the boundary conditions. The shape of the pressure profile also depends on the boundary conditions, becoming “steeper” as the initial capillary pressure becomes more negative; this has the effect of necessitating very small integration steps when the magnitude of the capillary pressure is large.

The most important relationship to be found from the results of these integrations is that between the boundary conditions $\hat{\psi}_w$ and $\hat{\psi}_i$ and the instantaneous flux per unit area at the wall, q . From Darcy’s law, this flux is equal to $(kk_r/\mu)\partial\psi/\partial x$, evaluated at

$x=0$. Using the chain rule, and the fact that $k_r=1$ when $x=0$ [since $\psi(x=0)\geq 0$], this can be written as

$$\begin{aligned}
 q &= \frac{k}{\mu} \frac{d\psi}{d\hat{\psi}} \frac{d\hat{\psi}}{d\eta} \frac{d\eta}{dx} \\
 &= \frac{k}{\mu} \frac{1}{\alpha} \frac{d\hat{\psi}}{d\eta} \left[\frac{\alpha(S_s - S_r)}{\beta t} \right]^{1/2} \\
 &= \left[\frac{\phi k (S_s - S_r)}{\mu \alpha t} \right]^{1/2} \left. \frac{d\hat{\psi}}{d\eta} \right|_{\eta=0} \quad (12)
 \end{aligned}$$

As is the case for a linear diffusion problem (such as fully-saturated flow), the instantaneous flux is proportional to $t^{-1/2}$. The constant of proportionality, which depends in a highly nonlinear way on both the potential at the wall and the initial capillary pressure, can be referred to as the "flux constant". The relationship between the (normalized) flux constant $d\hat{\psi}/d\eta|_0$ and the boundary conditions $\hat{\psi}_i$ and $\hat{\psi}_w$ is shown in Figure 4. As would be expected, the flux constant increases as either $\hat{\psi}_w$ increases or $\hat{\psi}_i$ decreases, since in either case there is an increase in the overall potential difference, which is the driving force for the flow. But whereas arbitrarily large values of $\hat{\psi}_w$ will lead to arbitrarily large fluxes, the flux constant rapidly approaches an asymptotic value as $\hat{\psi}_i \rightarrow -\infty$. This can be understood by noting that the flux is actually proportional not only to the potential drop, but also to the relative permeability; as $\hat{\psi}_i \rightarrow -\infty$, $S \rightarrow 0$ and $k_r \rightarrow 0$ (see Figure 1), so the excess flux due to the tail of the pressure profile is actually quite negligible.

Boundary-Layer Solution

For many purposes, it would be useful to have a closed-form solution that clearly illustrated the effect of the various parameters on the resultant flux. As explained before, there is no tractable method of exactly solving the governing equations (1-6). An extremely simple, albeit approximate, solution can be obtained, however, by using the so-called "boundary-layer", or "integral", technique. The boundary-layer method has been widely used for heat conduction problems [Goodman, 1964], heat transfer problems with phase change [Eckert and Drake, 1972], and hydrodynamic boundary-layer problems [Schlichting, 1968]. The method uses an assumed pressure profile that satisfies various boundary (or other subsidiary) conditions, but only satisfies the governing PDE in an integrated sense. If a reasonable trial function is assumed as the solution to the problem, the method is known to lead to accurate results for the types of problems previously mentioned.

The accuracy of the boundary-layer method for the present problem depends mainly on choosing an appropriate pressure profile; guided by the numerical results shown in Figure 3, this can be done as follows. First, consider a fixed but arbitrary time t , and note (from Figure 3) that the potential drops linearly from ψ_w at the wall down to zero at some distance λ into the formation. This part of the solution, representing the saturated flow, follows from equation (1) when k_r and S are constant. The pressure then drops, in a somewhat nonlinear manner, down to P_i . Although the capillary pressure, strictly speaking, does not reach ψ_i until $x \rightarrow \infty$, for practical purposes it can be considered to equal ψ_i for all $x > \lambda + \delta$, where δ and λ are penetration distances that each depend on t in some manner that is not known *a priori*.

It is clear from Figure 2 that ψ initially drops off linearly at the start of the unsaturated region, although it then becomes concave downward. Hence, $\psi(x = \lambda + \epsilon) = -a\epsilon + \dots$, where a depends on t , but not on ϵ . As will be seen below, however, it is much more convenient to utilize the saturation, rather than the

pressure, when integrating the equation in the unsaturated region. If the pressure profile has an initially linear variation, (2) can be used to show that the leading terms in the saturation profile must be of the form $S(x = \lambda + \epsilon) = S_s - b\epsilon^n + \dots$, where b depends on t , but not on ϵ . The simplest pressure and saturation profiles that satisfy the criteria just described are

$$\psi = \psi_w [1 - (x/\lambda)] \quad \text{for } 0 < x < \lambda, \quad (13)$$

$$S = S_s + (S_i - S_s) \left[\frac{x - \lambda}{\delta} \right]^n \quad \text{for } \lambda < x < \lambda + \delta, \quad (14)$$

$$S = S_i \quad \text{for } x > \lambda + \delta. \quad (15)$$

In any of the three regions, (2) could be used to relate ψ and S , if so desired, although it is convenient to use the pressure profile in the saturated region and the saturation profile in the unsaturated region. A relationship between the parameters λ and δ can be found by requiring the flux (and hence $\partial\psi/\partial x$) to be continuous at $x = \lambda$, which leads to

$$\lambda = (\alpha\psi_w) \left[\frac{m(S_s - S_r)}{(S_s - S_i)} \right]^{1/n} \delta. \quad (16)$$

It is usually recommended [Goodman, 1964] that trial profiles should have zero slope at the edge of the boundary layer, so that the flux is continuous at $x = \lambda + \delta$. While this condition is satisfied by the exact solution, since it merely reflects conservation of mass at the boundary between the disturbed and undisturbed zones, enforcing it

substantially complicates the algebraic manipulations that are needed to solve the problem, without a concomitant increase in the accuracy of the results. It is simplest to imagine that there is a small tail on the saturation profile expressed by equations (13-15), providing continuity of flux at the outer edge of the boundary layer, but sufficiently localized so as to make no perceptible contribution to the mass conservation integral.

With the pressure and saturation profiles given by equations (13-16), the conservation equation (1) is integrated from $x=0$ to $x=\infty$. Using the facts that $\partial\psi/\partial x=0$ for all $x > \lambda + \delta$, and $k_r = 1$ at $x=0$, the left side of (1) integrates out to

$$\int_0^{\infty} \frac{\partial}{\partial x} \left[\beta k_r(\psi) \frac{\partial \psi}{\partial x} \right] dx = -\beta \frac{\partial \psi}{\partial x} \Big|_{x=0} = \frac{\beta}{\alpha \delta} \left[\frac{(S_s - S_i)}{m(S_s - S_r)} \right]^{1/n} \quad (17)$$

Since $G(\psi) = dS/d\psi$, the right side of (1) equals dS/dt . To avoid a divergent integral (which would reflect the fact that the "infinite" half-space initially contains an infinite amount of liquid), S_i can be subtracted away from S ; this obviously will not affect the time derivative $\partial S/\partial t$. Hence the right side of (1) integrates out to

$$\begin{aligned} \int_0^{\infty} \frac{\partial}{\partial t} (S - S_i) dx &= \frac{d}{dt} \int_0^{\infty} (S - S_i) dx \\ &= \frac{d}{dt} \left\{ \int_0^{\lambda} (S_s - S_i) dx + \int_{\lambda}^{\lambda+\delta} (S_s - S_i) \left[1 - \left(\frac{x-\lambda}{\delta} \right)^n \right] dx + \int_{\lambda+\delta}^{\infty} (S_i - S_i) dx \right\} \\ &= \frac{d}{dt} \left[(S_s - S_i) \lambda + \int_0^1 (S_s - S_i) (1 - \zeta^n) \delta d\zeta + 0 \right] \end{aligned}$$

$$= (S_s - S_i) \frac{d}{dt} \left[\lambda + \frac{n}{n+1} \delta \right]. \quad (18)$$

Equating (17) and (18), and using (16) to express λ in terms of δ , leads to

$$\frac{\beta}{\alpha \delta} \left[\frac{(S_s - S_i)}{m(S_s - S_r)} \right]^{1/n} = (S_s - S_i) \left\{ \frac{n}{n+1} + (\alpha \psi_w) \left[\frac{m(S_s - S_r)}{(S_s - S_i)} \right]^{1/n} \right\} \frac{d\delta}{dt}. \quad (19)$$

Since none of the parameters appearing in equation (19) explicitly depend on δ or t , and since $\delta = 0$ when $t = 0$, (19) can be integrated to yield

$$\delta = \left[\frac{2kt}{\alpha \mu \phi} \frac{(S_s - S_i)^{-1+1/n}}{[m(S_s - S_r)]^{1/n}} \left\{ \frac{n}{n+1} + (\alpha \psi_w) \left[\frac{m(S_s - S_r)}{(S_s - S_i)} \right]^{1/n} \right\}^{-1} \right]^{1/2}. \quad (20)$$

The instantaneous volumetric flux at the wall is found by combining equations (16) and (20) with Darcy's law:

$$q = \frac{kk_r}{\mu} \left. \frac{\partial \psi}{\partial x} \right|_{x=0} = \frac{k}{\mu} \frac{\psi_w}{\lambda}$$

$$= \frac{k}{\mu} \frac{\psi_w}{[m(S_s - S_r)/(S_s - S_i)]^{1/n} \alpha \psi_w \delta}$$

$$= \left[\frac{k \phi}{2\alpha \mu t} \frac{(S_s - S_i)^{1+1/n}}{[m(S_s - S_r)]^{1/n}} \left\{ \frac{n}{n+1} + (\alpha \psi_w) \left[\frac{m(S_s - S_r)}{S_s - S_i} \right]^{1/n} \right\} \right]^{1/2}. \quad (21)$$

The pressure profiles predicted by the boundary-layer solution are compared to the essentially exact numerical solutions in Figure 5, for the cases where $n = 3$, $\hat{\psi}_w = 1$, and $\hat{\psi}_i = -1$ and -2 . The approximate solution not only correctly predicts that the flux is proportional to $t^{-1/2}$, it predicts the numerical value of the flux constant (which is proportional to the slope of the curve at the wall) quite accurately. The pressure profiles of the approximate solutions are similar to the exact profiles, with the agreement becoming poorer as the initial saturation decreases. This is to be expected, since the boundary-layer method does not explicitly account for the extreme variations in k_r that occur throughout the zone of penetration. Since the boundary-layer method does not utilize any information from the characteristic curves except the behavior of the capillary pressure curve (2) near $\psi = 0$, its accuracy is perhaps surprising. The overall accuracy of the boundary-layer method (in predicting the flux, for example), increases as ψ_w increases, since this method treats flow in the fully saturated zone *exactly*. Equation (21) is perhaps most useful in its display of the manner in which the various parameters influence the flux. While the fact that the flux is proportional to $(k/\mu t)^{1/2}$ can be predicted from dimensional arguments, the relative influences of ψ_i and ψ_w could not easily be seen *a priori*, and would probably require extensive numerical simulations to demonstrate. It is worth noting that (21) bears some resemblance to an exact solution derived by *Brutsaert* [1968] utilizing a more restrictive class of characteristic curves.

Example: Topopah Spring Welded Tuff

The unsaturated zone below Yucca Mountain in Nevada is being considered by the U.S. Department of Energy as a site for the construction of an underground repository for high-level radioactive waste [DOE, 1986; *Peters and Klavetter*, 1988; *Martinez*, 1988]. The Topopah Spring unit below Yucca Mountain is a welded volcanic tuff, with estimated values of porosity and absolute permeability of 0.14 and

$3.9 \times 10^{-18} \text{ m}^2$, respectively [Rulon *et al.*, 1986]. The van Genuchten parameters that have been found to provide the best fit to capillary pressure and relative permeability data from the Topopah unit are [Rulon *et al.*, 1986]: $S_s = 0.984$, $S_r = 0.318$, $n = 3.04$, $m = 0.671$, and $\alpha = 1.147 \times 10^{-5} \text{ Pa}^{-1}$. As an example of the use of the similarity transformation and boundary-layer methods for studying one-dimensional flow in unsaturated formations, horizontal flow from a saturated fracture in the Topopah unit will be treated.

Consider a vertical fracture that is saturated with water at zero potential, adjacent to a matrix which has an initial capillary pressure of $-1 \times 10^5 \text{ Pa}$ (-1 bar). (This capillary pressure is not meant to necessarily equal the *in situ* value at Yucca Mountain, but is chosen merely to illustrate the use of the two methods of solution). For times small enough so that the penetration thickness is less than half the distance to the nearest fracture, the "infinite half-space" assumption should be applicable. Using the parameters listed above for the Topopah welded unit, a fluid viscosity of 0.001 Pa s (1 cp), and an elapsed time of $1 \times 10^6 \text{ s}$ (11.6 days), the boundary-layer solution represented by (13-16) and (20) can be transformed into physical coordinates to give the pressure and saturation as a function of the distance from the fracture (Figures 6,7). The numerical solution of equations (9-11), likewise transformed from the similarity variables back to physical variables, is also shown in Figures 6 and 7. Since the instantaneous flux is proportional to the slope of the pressure profile at the wall, and the cumulative flux is proportional to the area under the saturation profile, it is clear that the two methods are in close agreement in this case. Note that this limiting case of zero boundary potential, in which there is no region of full saturation, is a "worst case" test of the boundary-layer method, since this method satisfies the governing equation (1) exactly in regions of full saturation.

As a further check of these two solutions, this problem has also been solved using TOUGH [Pruess, 1987], a finite-difference code that is known to produce accurate

results in problems involving the flow of water in porous and fractured media. The TOUGH solution (using 25 nodes spaced 0.04 m apart) agrees very closely with the solution based on the similarity transformation (Figures 6,7). As a comparison, Runge-Kutta integration of equation (9), including iteration to meet boundary condition (11), requires on the order of only 1% of the computational time needed to achieve similar accuracy with TOUGH, while the approximate boundary-layer method, which requires essentially no computer time, yields a cumulative flux that is accurate to within 10%. (Since TOUGH is a multi-purpose program that can also treat phase changes, heat transfer, formation compressibility, and other effects, this comparison is intended only to explain the usefulness of the present methods for this particular type of problem).

A main intended application of the approximate "boundary layer" solution is to calculate flow between fractures and matrix in the vicinity of the proposed nuclear waste repository at Yucca Mountain. The intention is to model the region using a numerical simulator such as TOUGH, with a mesh consisting only of "fracture elements". Equation (21) will be then used as a "source" or "sink" term for flow between the fractures and the adjacent matrix blocks. If successful, this approach will allow a considerable reduction in the number of elements required for accurate simulation, thereby reducing computational time and expense. The present solution would be useful for times that are small enough so that flow from one fracture is not affected by neighboring fractures. Application of this approach to longer time scales will be made possible by extending the "integral method" solution to other geometries, such as the cuboidal matrix blocks whose boundaries are formed by sets of intersecting fractures.

Conclusions

Two methods have been used to study one-dimensional flow of water in a semi-infinite, unsaturated porous media. In one method, the governing nonlinear PDE was transformed into an ODE by using a non-dimensionalized similarity variable, and then integrated numerically. The instantaneous flux was found to be proportional to $t^{-1/2}$, with a constant of proportionality that depends not only on the physical parameters of the medium, but also on the initial saturation and boundary pressure. The flux constant is an increasing function of the absolute values of both the potential at the boundary and the initial capillary pressure of the formation, although it reaches a finite asymptotic value for infinitely negative initial capillary pressures.

An approximate closed-form solution was also derived, using the "boundary-layer" approach. This solution correctly predicts all major qualitative features of the solution, including the $t^{-1/2}$ behavior of the instantaneous flux. The boundary-layer solution has an accuracy of (at worst) 15%, and explicitly shows the manner in which the boundary conditions and parameters of the characteristic curves influence the penetration distance and flux. The boundary-layer solution is currently being extended to deal with other problems of interest, such as flow into cuboidal matrix blocks whose boundaries are defined by sets of intersecting fractures.

Acknowledgments

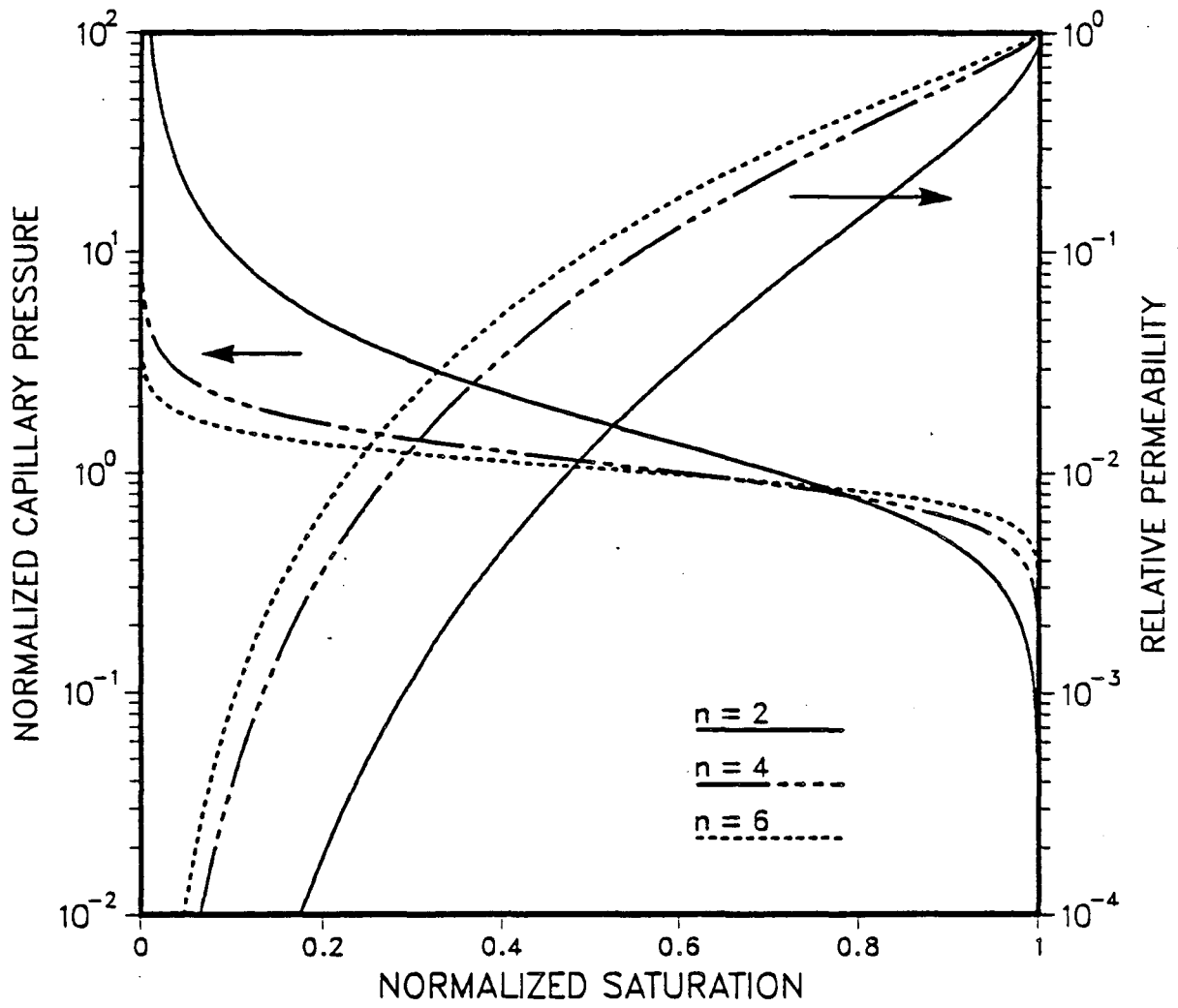
This work was carried out under U.S. Department of Energy Contract No. DE-AC03-76SF00098 administered by the DOE Nevada Office, in cooperation with the United States Geological Survey, Denver. The authors thank Dr. Karsten Pruess of Lawrence Berkeley Laboratory for making TOUGH available to them, and thank C. Doughty and J.S.Y. Wang (also of LBL) for reviewing this paper.

References

- Brutsaert, W., The adaptability of an exact solution to horizontal infiltration, *Water Resour. Res.*, 4, 785-789, 1968.
- Crank, J., *The Mathematics of Diffusion*, Oxford University Press, Oxford, 1975.
- Eckert, E.R.G., and Drake, R.M., Jr., *Analysis of Heat and Mass Transfer*, McGraw-Hill, New York, 1972.
- Goodman, T.R., Application of integral methods to transient nonlinear heat transfer, in *Advances in Heat Transfer, Vol. 1*, pp. 51-122, 1964.
- Hillel, D., *Fundamentals of Soil Physics*, Academic Press, New York, 1980.
- Martinez, M.J., Capillary-driven flow in a fracture located in a porous medium, *Rep. SAND84-1697*, Sandia Nat. Lab., Albuquerque, N.M., 1988.
- Peters, R.R., and Klavetter, E.A., A continuum model for water movement in an unsaturated fractured rock mass, *Water Resour. Res.*, 24, 416-430, 1988.
- Philip, J.R., General method of exact solution of the concentration-dependent diffusion equation, *Austr. J. Phys.*, 13, 1-12, 1960.
- Press, W.H., Flannery, B.P., Teukolsky, S.A., and Vetterling, W.T., *Numerical Recipes*, Cambridge University Press, Cambridge, 1986.
- Pruess, K., TOUGH user's guide, *Rep. LBL-20700*, Lawrence Berkeley Laboratory, Berkeley, Ca., 1987.
- Rulon, J., Bodvarsson, G.S., and Montazer, P., Preliminary numerical simulations of groundwater flow in the unsaturated zone, Yucca Mountain, Nevada, *Rep. LBL-20553*, Lawrence Berkeley Laboratory, Berkeley, Ca., 1986.
- Schlichting, H., *Boundary-Layer Theory, 6th Ed.*, McGraw-Hill, New York, 1968.

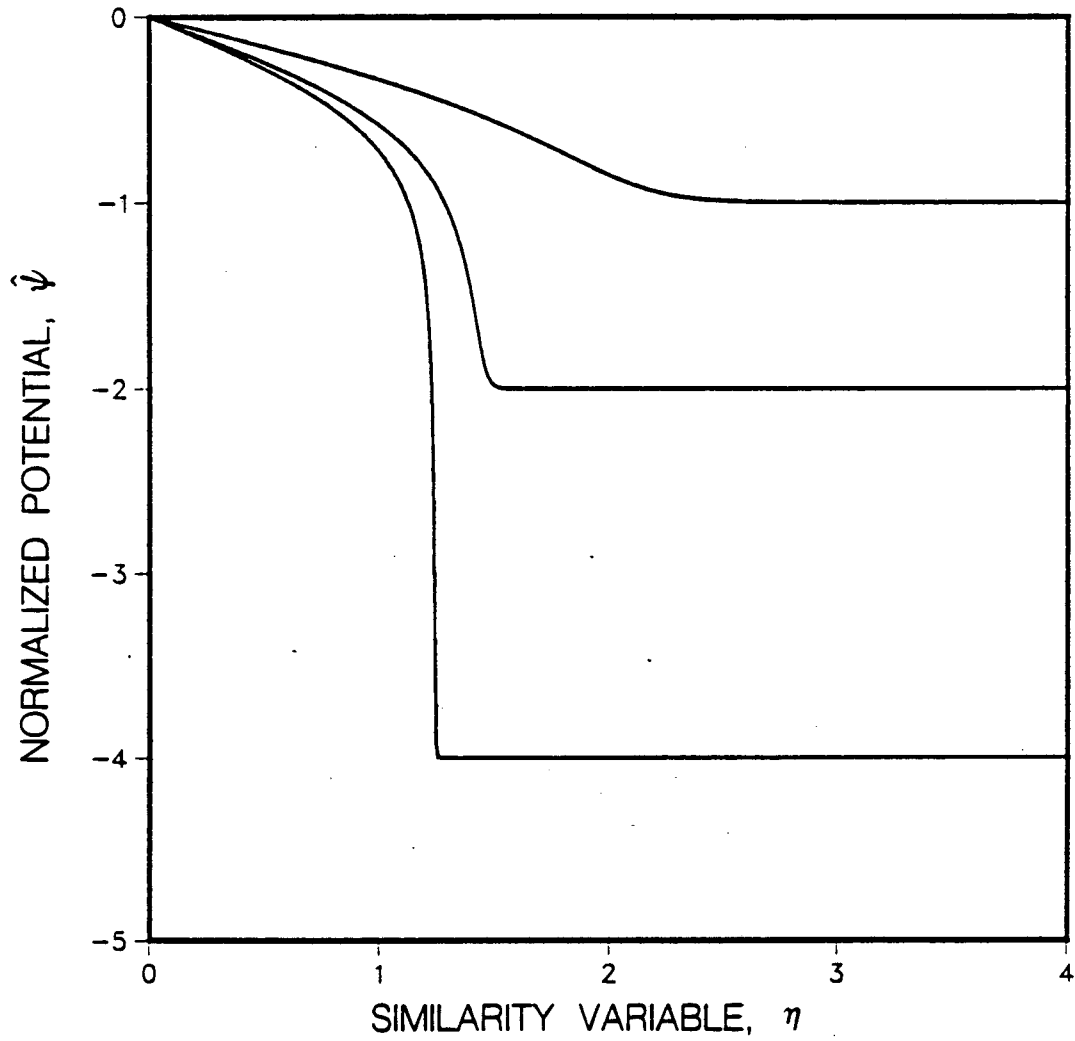
U.S. Department of Energy, Final environmental assessment - Yucca Mountain site, Nevada Research and Development Area, Nevada, *Rep. DOE/RW-0012*, Office of Civilian Radioactive Waste Management, Washington, D.C., 1986.

van Genuchten, M.T., A closed-form equation for predicting the hydraulic conductivity of unsaturated soils, *Soil Sci. Soc. Amer. J.*, 44, 892-898, 1980.



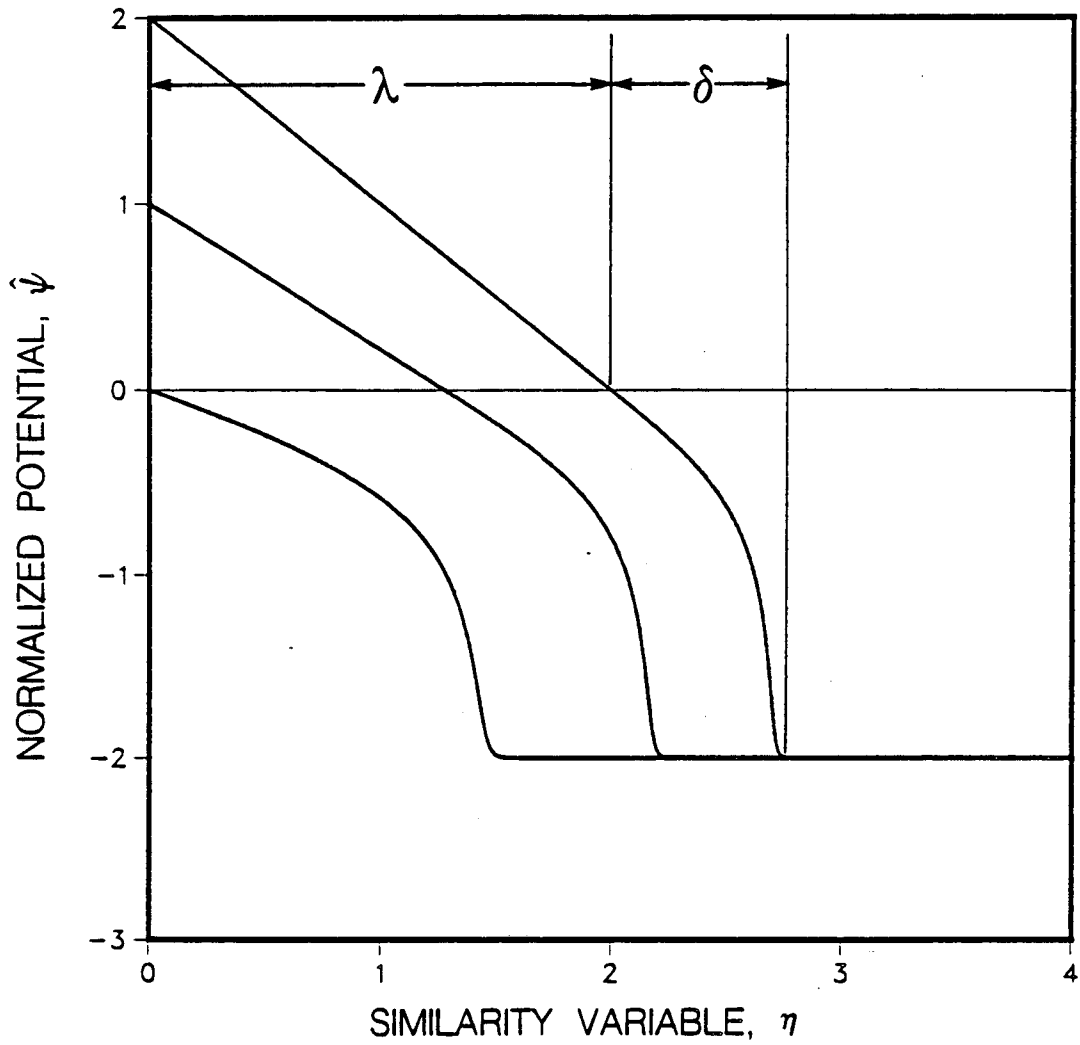
XBL 887-10338

Figure 1. Capillary pressure and relative permeability curves for media partially saturated with water, using the equations proposed by *van Genuchten* [1980]. After normalization, the shapes of the curves depend only on the parameter n .



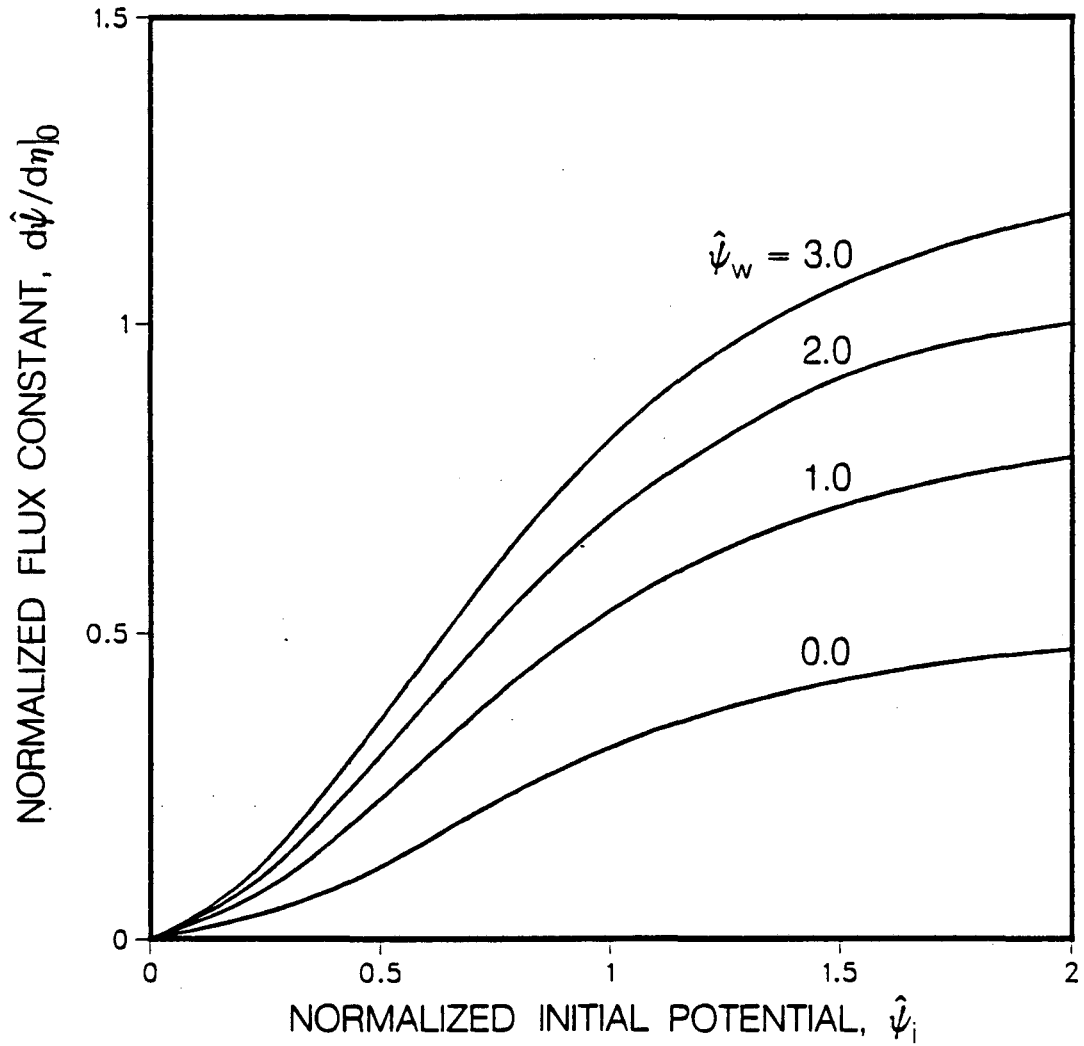
XBL 887-10337

Figure 2. Potential profiles for one-dimensional infiltration, with zero potential at the boundary, and various values of the initial capillary pressure. Profiles are derived from numerical solution of equation (9), using a value of $n = 3$.



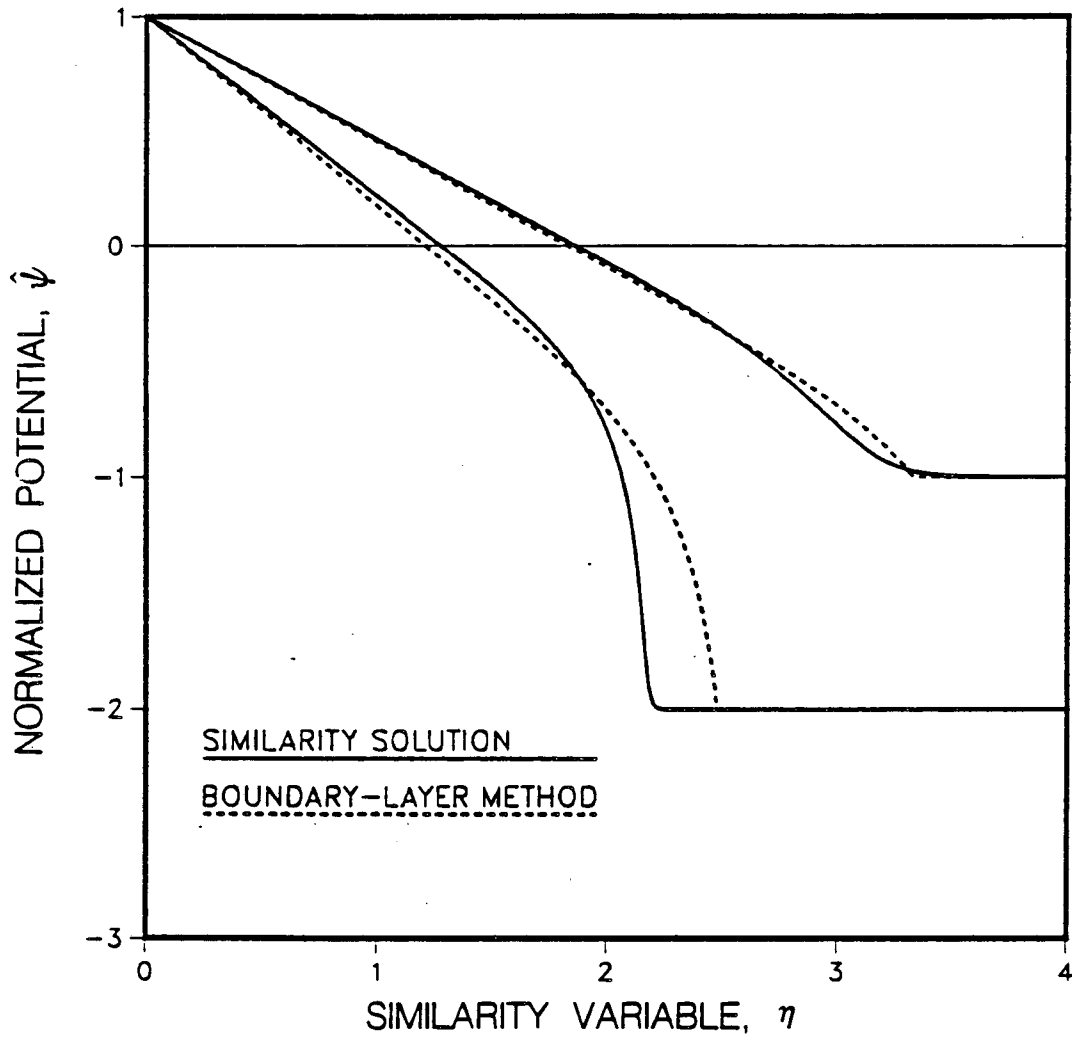
XBL 887-01336

Figure 3. Potential profiles for one-dimensional infiltration, for various values of boundary potential, and an initial normalized capillary pressure of -2. Profiles are derived from numerical solution of equation (9), using a value of $n = 3$. Penetration distances λ and δ are also shown.



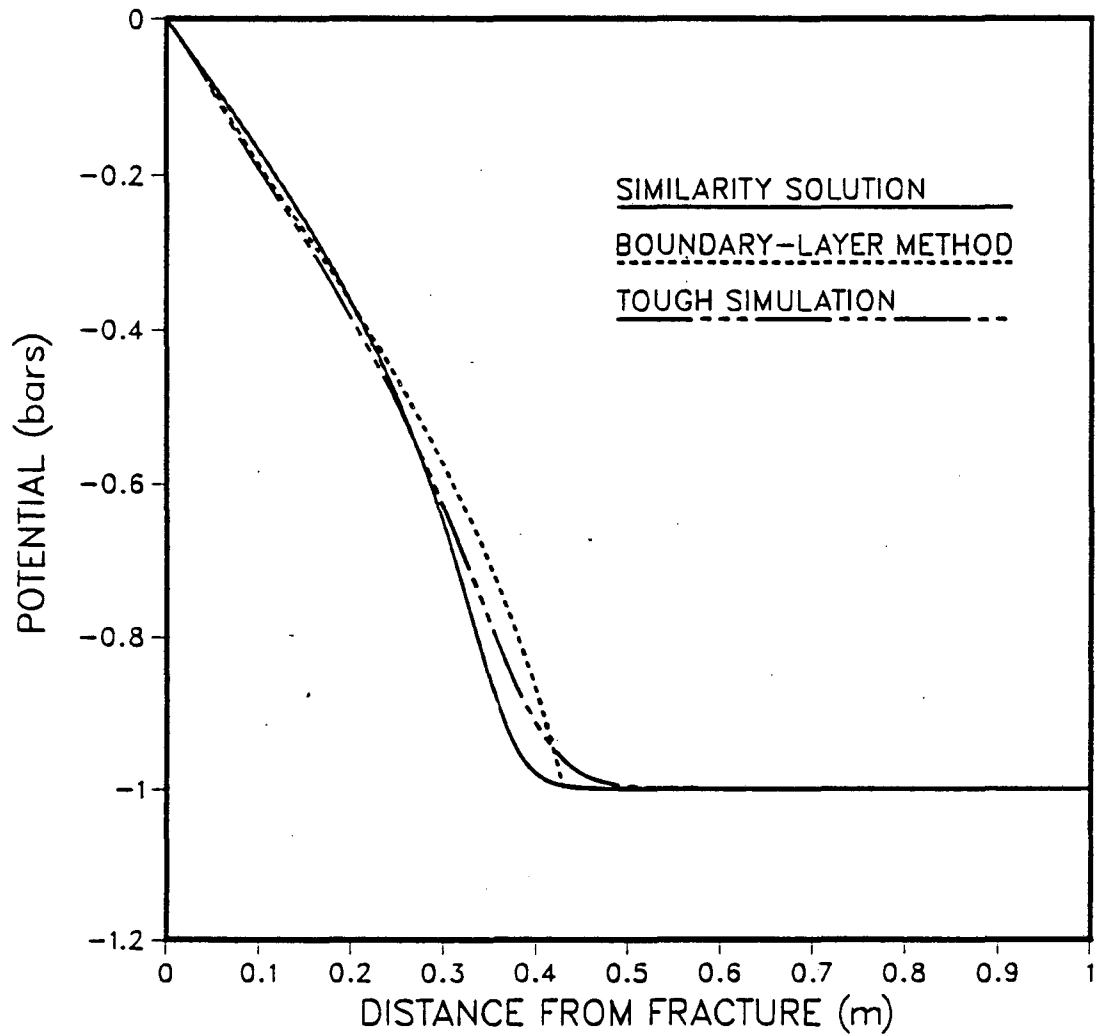
XBL 887-10335

Figure 4. Relationship between the flux constant and the boundary potentials. The potential at the wall is $\hat{\psi}_w$, and the initial capillary pressure in the medium is $\hat{\psi}_i$. Results are obtained from numerical solution of equation (9), using a value of $n = 3$.



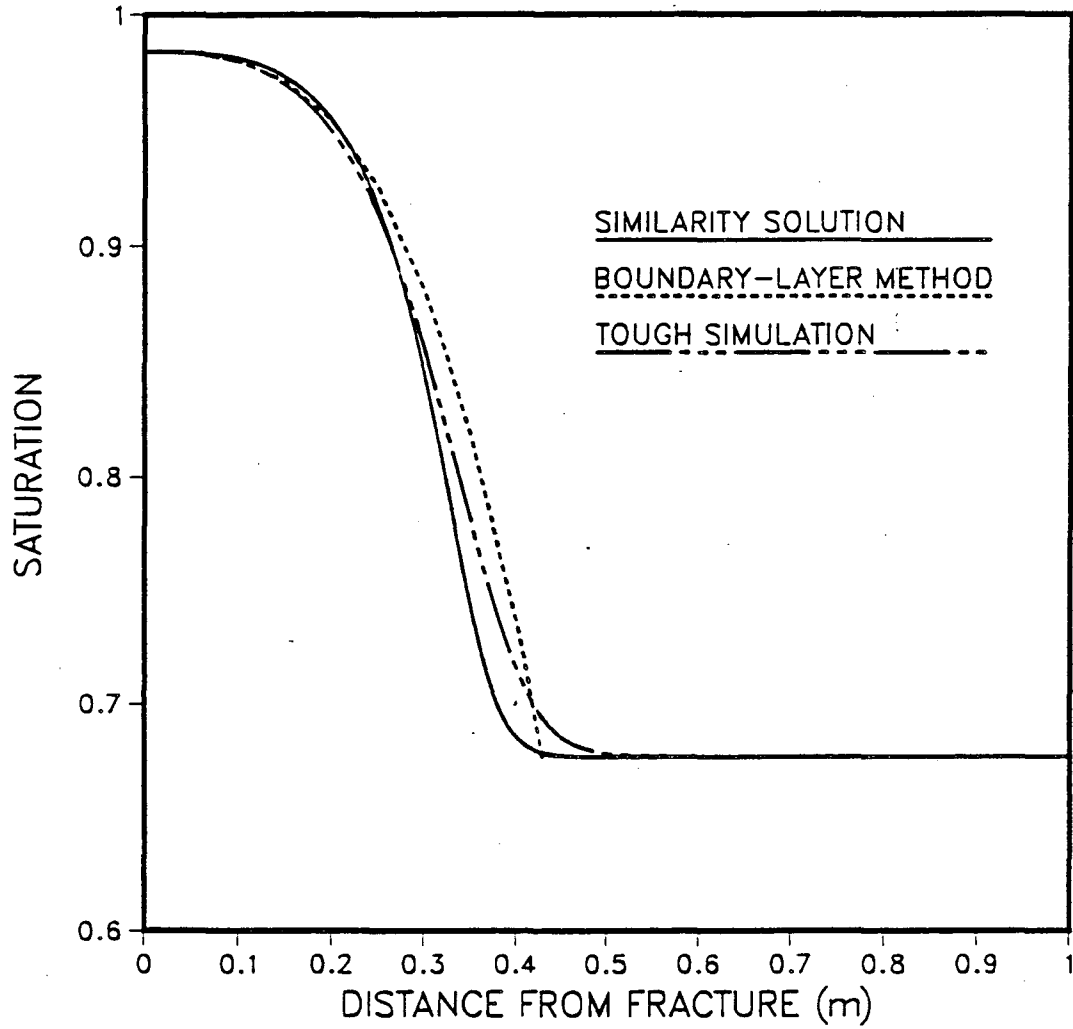
XBL 887-10334

Figure 5. Comparison of boundary-layer solution to the numerical solution of equation (9), using a value of $n = 3$. The normalized potential at the boundary is +1, and the initial normalized capillary pressures are -1 and -2.



XBL 887-10333

Figure 6. Pressure profile for influx into Topopah welded tuff formation, according to similarity solution, boundary-layer solution, and TOUGH simulation. The boundary potential is 0 bars, the initial capillary pressure is -1 bar, and the elapsed time is 1×10^7 seconds (116 days).



XBL 887-10332

Figure 7. Saturation profile for influx into Topopah welded tuff formation, according to similarity solution, boundary-layer solution, and TOUGH simulation. Boundary conditions and elapsed time are the same as in Figure 6.



*LAWRENCE BERKELEY LABORATORY
TECHNICAL INFORMATION DEPARTMENT
UNIVERSITY OF CALIFORNIA
BERKELEY, CALIFORNIA 94720*